Excitation-energy dependence of the mechanism for two-photon ionization of liquid H_2O and D_2O from 8.3 to 12.4 eV

Christopher G. Elles
Department of Chemistry, University of Southern California, Los Angeles, California 90089 and Chemistry Division, Argonne National Laboratory, Argonne, Illinois 60439

Askat E. Jailaubekov
Department of Chemistry, University of Southern California, Los Angeles, California 90089

Robert A. Crowell[a)]
Chemistry Division, Argonne National Laboratory, Argonne, Illinois 60439

Stephen E. Bradforth[b)]
Department of Chemistry, University of Southern California, Los Angeles, California 90089

(Received 4 April 2006; accepted 1 June 2006; published online 28 July 2006)

Transient absorption measurements monitor the geminate recombination kinetics of solvated electrons following two-photon ionization of liquid water at several excitation energies in the range from 8.3 to 12.4 eV. Modeling the kinetics of the electron reveals its average ejection length from the hydronium ion and hydroxyl radical counterparts and thus provides insight into the ionization mechanism. The electron ejection length increases monotonically from roughly 0.9 nm at 8.3 eV to nearly 4 nm at 12.4 eV, with the increase taking place most rapidly above 9.5 eV. We connect our results with recent advances in the understanding of the electronic structure of liquid water and discuss the nature of the ionization mechanism as a function of excitation energy. The isotope dependence of the electron ejection length provides additional information about the ionization mechanism. The electron ejection length has a similar energy dependence for two-photon ionization of liquid D_2O, but is consistently shorter than in H_2O by about 0.3 nm across the wide range of excitation energies studied. © *2006 American Institute of Physics*. [DOI: 10.1063/1.2217738]

I. INTRODUCTION

Radiation chemistry plays an important role in a wide variety of basic chemical sciences, from fundamental energy related fields, including solar power, nuclear power, and the hydrogen economy, to technological applications, such as plasma vapor deposition.[1] Processes that occur on the ultrafast time scale ($<10^{-11}$ s) determine to a large extent the outcome of radiation-induced chemical reactions, and knowledge of these dynamics is critical for developing an understanding of the basic mechanisms behind high energy chemical transformations. In particular, the ionization of liquid water and the chemistry of the resulting species play an important role in aqueous systems that are exposed to radiation. Ionization produces reactive intermediates that can, for example, damage biological molecules in living cells or generate dangerous amounts of hydrogen gas in radioactive waste storage tanks.[1] Radiolysis and photolysis experiments provide a window on the underlying chemistry in such systems by revealing information about the important reactions that occur following ionization in a controlled environment. Each ionization event produces a hydroxyl radical, a hydronium ion, and a solvated electron within the first few picoseconds, as in the case of two-photon ionization.

$$H_2O_{(aq)} + 2h\nu \rightarrow OH_{(aq)} + H_3O^+_{(aq)} + e^-_{(aq)}. \quad (1)$$

Although the kinetics of many important reactions involving these transient species are well known from research extending over the past several decades, a complete understanding of the ionization mechanism that produces them is still lacking. The mechanism is important because it determines the relative spatial distribution of the nascent species, which ultimately governs their subsequent chemistry.

One of the unresolved issues concerning the ionization mechanism in liquid water is how it changes with the excitation energy. At high enough excitation energies, where the electronic properties of water resemble those of an amorphous semiconductor, ionization potentially puts an electron into the conduction band of the liquid.[2,3] Thus, above some threshold it should be energetically possible to ionize a water molecule by exciting the electron directly into a quasi-free state in the conduction band, leaving the nuclear positions initially unchanged. The onset of this process is not well defined, but in this scenario the H_2O^+ cation subsequently decomposes by transferring a proton to a neighboring water molecule while the solvent traps and solvates the electron.[1] Although several estimates place the threshold energy for vertical ionization of liquid water in the range of 8.5–10 eV or higher,[2–6] photoionization can occur for excitation energies as low as 6.5 eV.[7,8] This discrepancy implies that nuclear motion of the excited water molecule plays a key role in the ionization mechanism at low excitation energies,

[a)]Electronic mail: rob_crowell@anl.gov
[b)]Electronic mail: bradfort@usc.edu

providing an alternate pathway for electron ejection that does not require direct (vertical) excitation into the conduction band of the liquid.[9] Several mechanisms have been proposed for excitation below the direct ionization threshold, but importantly, there is no clear and consistent picture of the ionization mechanism across this range of excitation energies. Furthermore, it remains unclear above what energy direct excitation into the conduction band plays the dominant role, how the mechanism changes with increasing energy up to that point, or exactly what is the nature of an electron in the conduction band of a disordered insulating liquid.

Understanding the mechanism of ionization and how it changes with increasing energy requires knowing the nature of the initially excited state and the underlying dynamics of the system. Theory does not currently provide a clear picture of the excited state in bulk water, or its energy dependence, but we expect that progress in this area will continue to shape our understanding of the mechanism. In the present experiments, we explore several aspects of the ionization process by measuring the geminate kinetics of the solvated electron at a series of excitation energies. The recombination kinetics of the electron provide insight into the ionization mechanism by revealing how far the electron initially separates from its geminate partners, OH and H_3O^+. The likelihood of recombination is a sensitive measure of this separation, often referred to as the thermalization distance or ejection length, because the greater the separation the less likely is geminate recombination. Quantitative models that account for the relative diffusion and reaction rates of the various species successfully reproduce the time-dependent survival probability of the electron following ionization, thus revealing the average electron ejection length, which is a key feature of the initial product distribution.[10,11]

An important result from previous measurements of the geminate recombination of the electron is that the survival probability, and therefore the ejection distance, strongly depends on the excitation energy. Work from a decade ago, using two-photon excitation to study total ionization energies in the range of 7.3–10.1 eV, showed that the average ejection length of electrons remains roughly constant below a threshold of about 9–9.5 eV, but increases significantly above that energy.[12] That paper also reports multiphoton ionization above 10.1 eV, via a proposed 3+1 multiphoton mechanism, but more recent work shows that the proposed 3+1 multiphoton ionization mechanism is not correct and that solvent heating by the high-intensity pump pulse influences the geminate kinetics.[13] Other experiments at excitation energies up to 10 eV support the observation that the ejection length increases rapidly above 9–9.5 eV,[6,14–21] although there are substantial difficulties in comparing previous results due to different methods of reporting recombination yields and the use of different fitting procedures. Further complicating that comparison is the fact that only a few authors specifically examine the energy dependence of the ionization mechanism over a broad range of energies,[6,8,12,14,15,22] and that, with the exception of a recent study at 12.4 eV by one of our groups,[21] there are no reliable data for excitation energies above 10 eV.

In the work described here, we fill the gap in experimental data and make a direct comparison with previous results by monitoring the geminate recombination of the electron after two-photon ionization at total energies between 8.3 and 12.4 eV in liquid water. Our results show that the average electron ejection length increases monotonically from a value of about 0.9 nm for excitation at 8.3 eV to about 3.8 nm at 12.4 eV. Comparing these results with ejection lengths measured following ionization of liquid D_2O suggests that the ejection length in D_2O is slightly, but consistently, shorter than in H_2O across this wide range of excitation energies. Isotopic substitution potentially provides additional insight into the ionization mechanism by revealing the relative influence of nuclear and electronic dynamics in the ionization process, but only a handful of previous studies examine the isotope dependence of ionization in liquid water.[6,21–25] We discuss the implications of our results for several possible ionization mechanisms in the context of recent liquid jet photoelectron experiments[26] and cluster ionization studies[2,3] that provide a framework for describing the electronic structure of water.

II. EXPERIMENT

We monitor the population of electrons following two-photon ionization of liquid water by observing the transient change in absorption at either 650 or 800 nm, where the electron is the only species that absorbs light.[27] Experiments with total excitation energies from 9.3 to 11.0 eV were performed at the University of Southern California, and measurements at 8.3 and 12.4 eV were made at Argonne National Laboratory. In the former experiments, corresponding to two-photon excitation from 267 to 225 nm, the excitation and probe laser pulses come from nonlinear frequency conversion of the 1 kHz output of a regeneratively amplified Ti:sapphire laser (Spectra Physics Hurricane). A hollow-core fiber containing argon gas generates tunable ultraviolet excitation pulses via four-wave mixing of the second harmonic of the Ti:sapphire laser with either the near-infrared light from an optical parametric amplifier (Spectra Physics OPA 800C) or the Ti:sapphire fundamental.[28] This is a useful new method for generating short, tunable pulses in the deep-ultraviolet region of the spectrum. Pumping the 10 cm long, 75 μm diameter fiber with about 80 μJ of 400 nm light and as much as 60 μJ of near-infrared light generates excitation pulses with up to 6 μJ of energy. A pair of matching calcium fluoride prisms compresses the pulses to a duration as short as 30 fs and a thin CaF_2 lens focuses them to a diameter of about 100 μm in the sample. An asynchronous chopper wheel modulates the signal by blocking the excitation beam with a frequency of about 300 Hz prior to the sample.

In order to obtain the 650 nm probe pulses, we generate continuum light by focusing a small portion of the Ti:sapphire fundamental into a sapphire substrate and then pass it through an interference filter with a center wavelength of 650 nm and a bandwidth of 20 nm. We focus the probe light to a diameter of less than 100 μm in the sample, where it intersects the excitation beam at a small angle. Referencing the intensity of the probe light after the sample to the frequency of the chopper wheel in a lock-in amplifier gives the

transient change in attenuation at 650 nm. Keeping the transient absorption below about 16 mOD ensures that the lock-in detection signal is linearly proportional to the change in absorbance and, therefore, the concentration of electrons. A gravity-drop jet creates the thin stream of liquid water in which the laser beams intersect.[29] We adjust the system to obtain a thickness of about 100 μm for H_2O, although the same parameters result in a slightly thicker jet of D_2O due to its higher density and viscosity.

The measurements at an excitation energy of 12.4 eV (two-photon excitation at 200 nm) were previously reported, as were details of the experiment.[21] A similar setup using that amplified Ti:sapphire laser system also gives the data at 8.3 eV, where the 3 μJ, 100 fs excitation pulses at 300 nm come from frequency quadrupling the signal light from an optical parametric amplifier (Spectra Physics OPA 800C). Similar to the above experiments, we obtain the probe pulses by generating continuum light in a 5 mm water cell and passing it through a 650 nm interference filter or by using the 800 nm fundamental of the laser directly. Overlapping the 100 μm diameter pump and 30 μm diameter probe beams in a 100 μm thick gear-pumped jet of liquid water while blocking every other pump pulse allows us to measure directly the transient absorption signal due to solvated electrons using shot-to-shot background subtraction.

The absorption strength changes quadratically with the excitation intensity in all of the experiments, indicating a two-photon process at each excitation energy. In addition to using neutral density filters to moderate the excitation pulse intensity, we also adjust the signal level by changing the excitation pulse duration, increasing the beam diameter at the sample, or changing the sample thickness, none of which affects the shape of the transient signal, only the magnitude. We use doubly purified H_2O with greater than 18 MΩ/cm resistivity and we use D_2O as received from either Cambridge Isotope Laboratories (99.9%) or Aldrich (99%). In the case of D_2O, we confirm the isotopic purity of the sample to better than 3% by accurately measuring the density before and after use. Deaerating H_2O by continuously bubbling nitrogen gas through the liquid does not change the transient signal, verifying that the oxygen that is naturally dissolved in water does not affect our measurements.

III. RESULTS AND ANALYSIS

Figure 1 shows the transient signal following photoionization of liquid water at several excitation energies from 8.3 to 12.4 eV. The change in absorption over the first few picoseconds (not visible in the figure) is primarily a result of the spectral shift that accompanies solvent reorganization around the electron and depends on the probe wavelength.[30,31] Because the spectral shift does not correspond to population dynamics, we consider only the data for delays longer than 5 ps, after which the shape and position of the electron spectrum remain constant and the signal amplitude reflects the concentration of solvated electrons. All of the traces decay nonexponentially to a fraction of their maximum amplitude, with the amount of decay depending on the excitation energy. At the lowest energy, the signal decays to less than half of its maximum amplitude by 1 ns, while the signal for higher excitation energies decays by as little as about 15% over the same period of time. The traces in the figure are the averages of several sets of data at each wavelength, and we normalize each trace by extrapolating the signal to a delay of 0 ps using the model described below. Collecting multiple sets of data on different days minimizes the influence of systematic drift in the signal that comes from subtle changes in the experimental setup. Although these effects are small, they are the limiting factor in the accuracy of our measurements, which is given by the uncertainty in the fits to the data (see below).

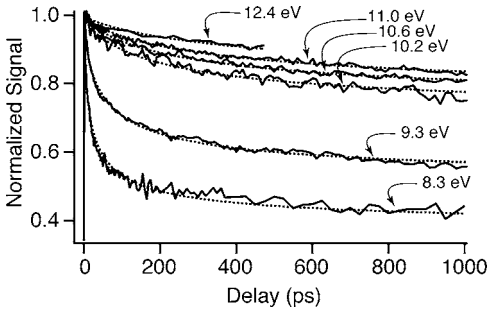

FIG. 1. Transient absorption signal for two-photon ionization of liquid H_2O at several excitation energies. The dotted lines are fits to the data using the IRT/IP model.

A. Kinetic model

The dotted lines in Fig. 1 are fits to the data using a model that accounts for the decay of electrons due to geminate recombination with the hydroxyl radical and hydronium ion partners.

$$OH_{(aq)} + e^-_{(aq)} \rightarrow OH^-_{(aq)}, \tag{2}$$

$$H_3O^+_{(aq)} + e^-_{(aq)} \rightarrow H_2O_{(aq)} + H_{(aq)}. \tag{3}$$

The model, alternately called the independent reaction times[10] (IRT) or the independent pairs[11] (IP) model, assumes that the competing recombination reactions proceed independently, and that the joint survival probability of the electron Ω is equal to the product of the survival probabilities for each individual reaction ($\Omega = \Omega_{OH} \cdot \Omega_{H_3O^+}$). The framework for describing the time-dependent survival probability of an electron as a function of its ejection length r_0 is described separately by Pimblott[11] and by Goulet and Jay-Gerin.[10] Although these authors use slightly different approaches, the result is the same in both derivations, with the primary difference between their methods being the way that they obtain the time-dependent population of electrons $P(t)$ for a given spatial distribution of the hydroxyl radical, hydronium ion, and electron. Both methods require sampling many discrete configurations of the initial distribution in order to obtain the ensemble average of $P(t)$, for which there is no analytical solution.

An alternate method of obtaining the population of electrons as a function of time is to numerically integrate the joint survival probability function over the initial distribution of electrons $f(r_0)$.[18–20]

TABLE I. Parameters for the independent reaction time/independent pair (IRT/IP) model. All values are taken from Ref. 21. The values come from experimental diffusion and reaction rate measurements, except for the reaction of electrons with OD, where it is assumed that the reaction radius is the same as in the nondeuterated reaction, and that the diffusion constant of the hydroxyl radical scales with the viscosity (~20% slower for OD in D_2O than OH in H_2O).

	R_{OH,e^-} (nm)	D_{OH,e^-} (nm^2/ns)	$R_{H_3O^+,e^-}$ (nm)	$D_{H_3O^+,e^-}$ (nm^2/ns)	$v_{H_3O^+,e^-}$ (nm/ns)
H_2O	0.54	7.7	0.50	13.9	4.0
D_2O	0.54	6.1	0.50	10.6	1.5

$$P(t) = \int_R^\infty \Omega(r_0,t) f(r_0) 4\pi r_0^2 dr_0. \tag{4}$$

The lower limit of integration is equal to the radius at which electrons react with either OH or H_3O^+, because electrons initially formed within that radius are assumed to react immediately without contributing to the signal that we measure. The integration ignores the initial separation of the hydroxyl radical and the hydronium ion by implicitly assuming that they are both at the origin of the electron distribution. Neglecting the separation of the molecular species is a valid approximation when that distance is small relative to the distribution of electrons. Accordingly, Pimblott[11] shows that including an initial separation of 0.3 nm, approximately the width of one solvation shell, between the hydroxyl radical and the hydronium ion has very little effect on the overall kinetics for an electron distribution with an average ejection length of 1.0 nm.

Numerical integration has the advantage of allowing us to fit the data directly using a least-squares routine, rather than visually estimating the best fit from a series of precalculated decay curves, as is often done.[10,11] Using an initial radial distribution of electrons with the form of either a Gaussian function,

$$f(r_0) = \frac{\exp(-r_0^2/2\sigma^2)}{\sqrt{8\pi^3\sigma^6}}, \quad \langle r_0 \rangle = \sigma\sqrt{8/\pi}, \tag{5}$$

or an exponential function,

$$f(r_0) = \frac{\exp(-r_0/b)}{8\pi b^3}, \quad \langle r_0 \rangle = 3b, \tag{6}$$

the average ejection length $\langle r_0 \rangle$ and the initial amplitude $P(t=0)$ are the only parameters that vary in our fits to the data. We use the values in Table I for the remaining parameters, which are the joint diffusion constant (D_{OH,e^-}) and reaction radius (R_{OH,e^-}) for recombination of the electron with the hydroxyl radical, as well as the diffusion constant ($D_{H_3O^+,e^-}$), reaction radius ($R_{H_3O^+,e^-}$), and reaction velocity ($v_{H_3O^+,e^-}$) for recombination with the hydronium ion.[21] In addition to giving the average ejection length, our fits to the data reveal the ultimate electron survival probability by extrapolating to the value $P(t=\infty)$ at infinite delay. Table II lists the average ejection lengths and extrapolated survival probabilities that we obtain by fitting our data for the ionization of liquid H_2O. The uncertainties that we report are two standard deviations from the average value that we obtain by fitting several independent traces at each excitation energy.

TABLE II. Electron ejection lengths and survival probabilities for H_2O. Uncertainties are two standard deviations.

	Gaussian distribution		Exponential distribution	
Excitation Energy (eV)	$\langle r_0 \rangle$ (nm)	Survival probability[a] (%)	$\langle r_0 \rangle$ (nm)	Survival probability[a] (%)
8.3	0.9(0.2)	36(6)	0.8(0.2)	33(6)
9.3	1.4(0.2)	50(4)	1.3(0.2)	47(4)
10.2	2.4(0.4)	66(5)	2.5(0.5)	65(5)
10.6	3.0(0.3)	72(2)	3.3(0.4)	71(3)
11.0	3.2(0.3)	74(2)	3.5(0.4)	73(3)
12.4	3.8(0.6)	77(3)	4.5(0.8)	78(4)

[a]Extrapolation of the geminate recombination model function to infinite delay.

The appropriate form of the distribution function depends on the ionization mechanism and is generally assumed to be either a Gaussian or an exponential function. Similar to previous reports,[10–12,19,20] we find that using either of these distribution functions for the initial ejection length fits the data equally well at all excitation energies. Additionally, the wide range of energies in our study allows us to test systematically how the choice of distribution function affects the values of $\langle r_0 \rangle$ that come from fitting the data. Both the Gaussian and exponential distributions give similar $\langle r_0 \rangle$ for intermediate energies, but the value from the exponential distribution, relative to the value from a Gaussian distribution, systematically shifts from about 15% smaller at an ionization energy of 8.3 eV to nearly 20% larger at 12.4 eV (see Table II). This trend highlights a weak sensitivity of the fit to the shape of the distribution, but does not reveal any physical characteristic of the system. The choice of distribution function only affects the value of $\langle r_0 \rangle$ for excitation energies at the limits of our energy range, where the distribution is either very narrow or very broad, whereas most previous measurements are in the intermediate range, and that choice has only a small impact on the fitting parameter. We use a Gaussian distribution function for all of our data, except where otherwise noted.

B. Electron ejection length and survival probability

Figure 2 shows our results for the average ejection length $\langle r_0 \rangle$ in liquid water as a function of the excitation energy, along with data from several previous experiments. The closed circles are our values, the open diamonds are from Crowell and Bartels,[12] and the open circles are from various other sources,[6,18–20,25,32] as listed in Table III. The data in the inset are from a series of measurements at intervals of approximately 0.1 eV in the excitation range of 10.1–10.7 eV. In order to facilitate a comparison of our results with those in the literature, we include only data points obtained from the IRT/IP model. The most common alternative in the literature is a simple survival probability model that takes the form of the complementary error function,[14,32] and it essentially approximates the geminate kinetics of the

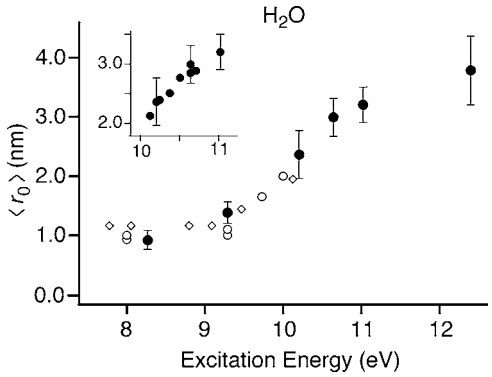

FIG. 2. Average electron ejection length as a function of excitation energy for two-photon ionization of H_2O. The closed circles are the average value that we obtain from fitting the IRT/IP model to several traces at each energy, with the error bars representing two standard deviations from the mean. The open markers are data from various other sources (see Table III).

electron as a single diffusion-limited recombination reaction with a δ-function initial distribution. The simple model tends to overestimate the survival probability, because it generally fits the data poorly at short delay times, and does not provide a quantitative estimate of the electron ejection length. As mentioned in the Introduction, we exclude data points from Ref. 12 that were originally assigned to a 3+1 resonant multiphoton ionization mechanism, because a more recent study suggests that solvent heating by the intense pump laser influences the recombination kinetics in those traces.[13]

We also measure the kinetics of the solvated electron following two-photon ionization of deuterated water. Figure 3 compares a series of electron decay curves for H_2O and D_2O, excluding for clarity the traces that we obtain at an excitation energy of 10.6 eV. The decay of the normalized signal is nearly identical in each liquid at the higher ionization energies (10.2–12.4 eV), but, in contrast, the signal decays more in D_2O than it does in H_2O after ionization at 8.3 and 9.3 eV. The geminate kinetics depend on the diffusion and reaction rates of the recombining species, which are

TABLE III. Electron ejection lengths from literature sources using the IRT/IP model.

Energy (eV)	$\langle r_0 \rangle$ (nm) H_2O	$\langle r_0 \rangle$ (nm) D_2O	Distribution function	Source
10.1	2.0		Gaussian	Reference 12
10.0	2.0[a]	1.7[a]	Gaussian	Reference 6
9.7	1.7		Exponential	Reference 20
9.5	1.6		Gaussian	Reference 12
9.3	1.1		Exponential	Reference 18
9.3	1.0		Exponential	Reference 19
9.1	1.2		Gaussian	Reference 12
8.8	1.2		Gaussian	Reference 12
8.1	1.2		Gaussian	Reference 12
8.0	1.0	1.0	Gaussian	Reference 25
8.0	0.9[b]		Gaussian	Reference 11 and 32
7.8	1.2		Gaussian	Reference 12

[a]Determined from the reported survival probabilities of 0.62 in H_2O and 0.59 in D_2O using the IRT/IP model.
[b]Value reported in Ref. 11 for the data in Ref. 32.

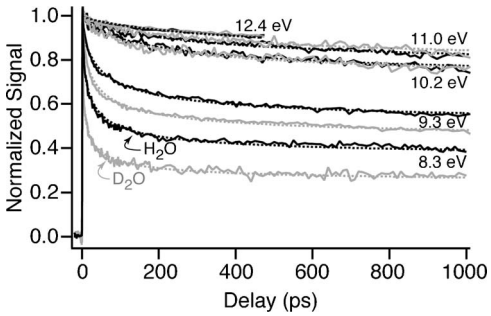

FIG. 3. Transient absorption signal for two-photon ionization of liquid H_2O (black curves) and D_2O (gray curves) at several excitation energies. Dotted lines are fits to the data using the IRT/IP model with the appropriate parameters from Table I.

slightly different in the two liquids, and therefore do not directly reveal the influence of isotopic substitution on the initial ionization event. Instead, the value of $\langle r_0 \rangle$ is a more direct indicator of the isotope dependence because the IRT/IP model accounts for the different rates in each liquid. Fitting the data with the IRT/IP model and the appropriate parameters in Table I allows us to quantitatively compare the results in each solvent.[33]

Figure 4 shows the average ejection length and survival probability for H_2O and D_2O as a function of energy. The circles in the figure are our data, while the squares at 8 eV are from Crowell and Bartels,[25] and those at 10 eV are from Sander *et al.*[6] Two earlier papers[23,24] also compare the kinetics in H_2O and D_2O following 8 eV excitation and find qualitatively the same result as Crowell and Bartels, but they use a simple error function to model the geminate decay that does not facilitate a quantitative comparison with our results. Interestingly, the isotope dependence that we observe is simi-

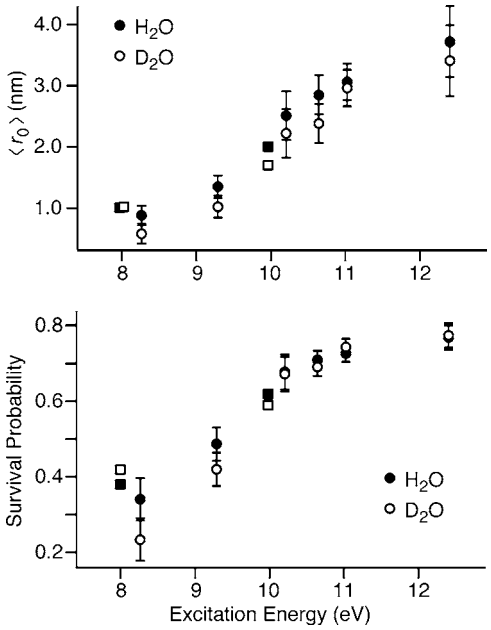

FIG. 4. Average ejection length (top panel) and ultimate survival probability (bottom panel) as a function of the excitation energy for two-photon ionization of H_2O (closed circles and squares) and D_2O (open circles and squares). The circles are our data, the squares at 8 eV are from Ref. 25, and the squares at 10 eV are from Ref. 6.

lar to the previous measurement at 10 eV excitation, but contrasts with the measurements at 8 eV, where there is more recombination in H_2O than in D_2O. Crowell and Bartels[25] suggest that the different diffusion constants and reaction rates almost entirely account for the different kinetics that they observe at 8 eV and that the ejection lengths are nearly the same in each liquid. In contrast, our results from 8.3 to 12.4 eV, as well as those of Sander *et al.*[6] at 10 eV, show that the ejection length is consistently shorter by about 0.3 nm in D_2O than in H_2O.

The previous experiments[23–25] at 8 eV measure the electron kinetics for only 90 ps or less following ionization, whereas our measurements extend to 1 ns and capture more completely the important kinetics. Measuring the decay of electrons for longer delays gives more robust parameters from fitting the data, which, in turn, allows for more accurate extrapolation of the signal to zero delay and to the long time limit. It is also possible that the previous data for 8 eV excitation overestimate the survival probability, and therefore the ejection length, in D_2O due to a contribution from three-photon absorption or from solvent heating by the pump pulse. Pumping the sample with high power laser pulses in order to obtain good signal levels often produces these unwanted nonlinear effects,[13,34] especially at low excitation energies where the ionization yield is very small ($<5\%$).[22] Nonlinear effects may have a more pronounced influence on the signal in D_2O, because the ionization yield is smaller in that liquid than in H_2O,[22] but the 300 nm excitation pulses in our experiment are too weak for us to test this hypothesis for an excitation energy of 8.3 eV. Nonetheless, we have made a consistent measurement over a wide range of energies in order to compare the isotope dependence, giving us a more complete data set than was previously available.[35]

IV. DISCUSSION

The collection of data points in Fig. 2 confirms the earlier observation that the electron ejection length in liquid water remains nearly constant with increasing excitation energy below about 9–9.5 eV and then starts to increase rapidly for excitation energies up to 10.1 eV.[12] Our data also extend those results to higher energies, showing that the average ejection length continues to increase monotonically up to at least 12.4 eV. The data in the inset show that the increase is smooth from 10 to 11 eV and that there is no resonance or other structure in the electron ejection "action spectrum" in this range. The more dramatic increase of the ejection length starting around 9.5 eV roughly coincides with the second electronic absorption band and with the onset of vertical electronic excitation into the conduction band of liquid water (see below). We discuss the spectroscopy and important energy levels of the liquid and then consider how our results connect with the energy dependence of the ionization mechanism.

A. Electronic structure of liquid water

Figure 5 highlights a few of the important vertical transition energies for water that come from the one- and two-photon absorption spectra[18,36] and the photoelectron spectrum[26] of the liquid. The absorption spectra give the vertical transition energies to the first two excited states, $\tilde{A}\ ^1B_1$ and $\tilde{B}\ ^1A_1$, and indicate the presence of several overlapping transitions at higher energy. The first two excited states, which are both dissociative in the gas phase,[37] are a result of one-electron transitions from the $1b_1$ nonbonding and $3a_1$ bonding orbitals, respectively, to the initially unoccupied $4a_1$ orbital.[38,39] The upper $4a_1$ orbital, which is the same in each transition, is often described as an oxygen $3s$ Rydberg orbital.[4] Several narrow absorption bands arising from transitions to higher Rydberg orbitals ($3p$, $3d$, etc.) dominate the gas phase spectrum of water (not shown) above the $\tilde{B}$ state,[38] but these are not resolved in the liquid spectrum. Although a similar increase in the density of states should also exist for the liquid in this energy regime up to the corresponding liquid phase ionization potentials, the energies and precise character of Rydberg states in the bulk liquid are not currently understood,[39] and therefore they are not shown in the energy level diagram in Fig. 5(c). An interesting difference between the one- and two-photon absorption spectra is the relative intensity of the transitions to the first and second excited states. Contrasting with the one-photon spectrum, which has a strong absorption maximum at 8.2 eV, the $\tilde{A}$ band in the two-photon spectrum is much weaker than the second absorption band, with the two-photon spectrum decreasing by an order of magnitude or more in this region.[8,18] The relatively weak two-photon transition probability to the $\tilde{A}$ state may originate from the atomic oxygen $s \leftarrow p$ character of the excitation, even though the two-photon molecular transition is not strictly symmetry forbidden.[40] We are currently study-

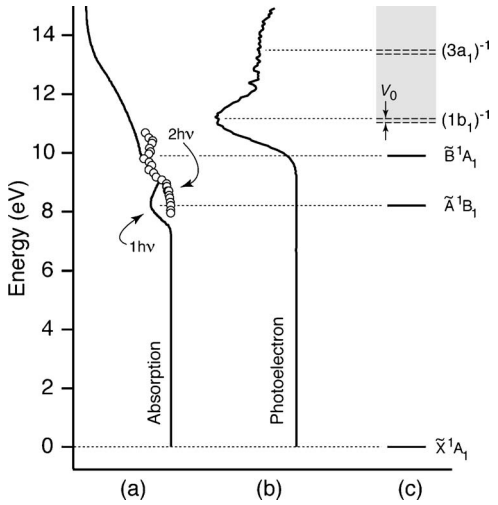

FIG. 5. Spectroscopy [(a) and (b)] and vertical transition energies (c) of liquid water. The one- and two-photon absorption spectra (panel a; reproduced from Refs. 36 and 18, respectively) give vertical transition energies for the first two excited states, $\tilde{A}$ and $\tilde{B}$. The peak at 11.2 eV in the photoelectron spectrum of bulk water (panel b; reproduced from Ref. 26) defines the vertical binding energy with respect to vacuum for electrons in the $1b_1$ highest occupied molecular orbital. The energy for a direct transition to the conduction band of the liquid differs from the energy for ejecting an electron into vacuum by V_0. Here, we use the value $V_0=-0.12$ eV in Ref. 2, which comes from extrapolating ionization data for water clusters to the bulk liquid.

ing the ionization and dissociation yields in this region in an effort to clarify the nature of the excited state created by two-photon absorption at 8.3 eV.

The photoelectron spectrum in Fig. 5(b) shows the binding energies for electrons in liquid water, with the band at 11.2 eV corresponding to the removal of electrons from the $(1b_1)$ highest occupied molecular orbital.[26] The energy of the band maximum is the most probable transition energy for vertical excitation of an electron from the equilibrium ground state of a liquid water molecule into the vacuum, without giving it any excess kinetic energy. (The probing depth in the liquid microjet experiments is 1–2 nm and therefore most electrons reaching the vacuum come from water in bulklike environments.[26,41]) Nonequilibrium ground state geometries and different solvent configurations (e.g., hydrogen-bonding coordination) contribute to the width of the peak in the photoelectron spectrum. Such poorly solvated water configurations give rise to the lower energy onset of the photoelectron band, at about 9.9 eV, providing an estimate of the minimum energy for optically accessible direct ionization into the vacuum.[26] This value is consistent with the older photoemission "threshold" reported by Delahay and Von Berg,[42] although in this situation there is no proper threshold, but rather an exponentially decaying tail due to diminishing Franck-Condon overlap between the initial and final solvent states.[3]

In contrast with the ejection of photoelectrons into the vacuum, the vertical ionization energy for exciting an electron into the conduction band of the liquid depends on how much solvent polarization stabilizes (or destabilizes) an electron in the conduction band relative to the vacuum. There is some debate about the extent of this solvent stabilization energy V_0, which is compounded by confusion in the literature concerning the use of adiabatic versus vertical band-gap energies. One commonly cited estimate for V_0 is −1.2 eV,[5] but a recent and thorough analysis of the problem by Coe *et al.*[2,3,43,44] that extrapolates cluster ionization data toward bulk quantities suggests that the magnitude of V_0 is much smaller, lying in the range from −0.12 to 0.0 eV. (An extrapolation of *ab initio* calculations for water clusters also supports the latter range.[45]) Combining the newer estimate for V_0 and the vertical transition energy from the photoelectron spectrum in Fig. 5(b) gives a most probable transition energy between 11.1 and 11.2 eV for promoting an electron directly from the top of the valence band to the conduction band without giving the electron any excess energy. (Accordingly, the onset of direct ionization by vertically exciting an electron from a nonequilibrium, but significantly populated, ground state water configuration into the conduction band of the liquid is about 9.8–9.9 eV, depending on the value of the solvent stabilization energy V_0.) The conduction band is accessible indirectly for lower excitation energies as well, but only after nuclear rearrangement of the excited molecule and surrounding solvent. To illustrate this point, an approximate energy level diagram in Fig. 6 depicts several of the relevant energies for ionizing liquid water, including the most probable vertical excitation energies from Fig. 5 (left), the energy of the equilibrium solvated electron and ionization products (right), and the adiabatic bottom of the conduction band (middle).[1–3]

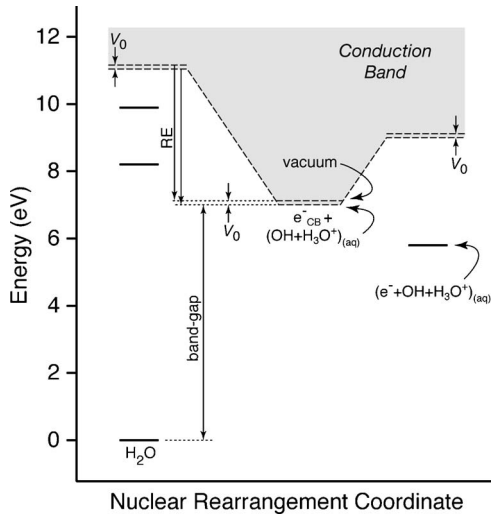

FIG. 6. Schematic energy level diagram for liquid water (based on Refs. 1–3). The energy levels at the left are for vertical transitions from the equilibrium ground state of the liquid, as in Fig. 5, and those at the right are for vertical excitation of an equilibrium solvated electron. At the middle of the diagram is the adiabatic bottom of the conduction band, defined as the minimum energy of an electron delocalized in the conduction band with all other species fully relaxed. The adiabatic bottom of the conduction band is separated from the adiabatic vacuum level by V_0, where the adiabatic vacuum level is defined similarly (i.e., a zero kinetic energy electron in vacuum with the other species fully solvated and relaxed). V_0 is assumed constant across the diagram. The adiabatic energies and the value for V_0 shown are based on extrapolation of cluster data to the bulk in Ref. 2. The total reorganization energy (RE) is the difference from the nonequilibrium configuration around the nascent H_2O^+ to the fully solvated OH and H_3O^+ products of the deprotonation reaction following ionization. The bottom axis therefore represents a generalized nuclear rearrangement coordinate that includes both the proton transfer coordinate and rearrangement of the surrounding water network.

The diagram highlights the importance of nuclear reorganization when considering the energetics of ionizing liquid water and shows that the adiabatic bottom of the conduction band is well below the vertical transition energy for reaching the conduction band from the equilibrium ground state.[2,3] The adiabatic bottom of the conduction band by definition contains a quasi-free electron with minimal kinetic energy and with all other species and the solvent fully relaxed $(e^-_{CB}+OH_{(aq)}+H_3O^+_{(aq)})$. As H_2O^+ is unstable with respect to proton transfer to neighboring water molecules,[46] the fully relaxed form of the ionized solute is the separated hydroxyl radical and hydronium ion, and the total reorganization energy (RE) is therefore the difference from the vertically prepared, highly nonequilibrium configuration around the nascent H_2O^+ to the fully solvated $OH_{(aq)}$ and $H_3O^+_{(aq)}$ products. Further nuclear rearrangement occurs when the solvent traps an electron from the conduction band to form a solvated electron $(e^-_{(aq)})$. The lowest state on the right side of the figure is the energy of the fully relaxed ionization products, including the fully solvated electron, and it is the population of this state, formed within a few picoseconds of ionization regardless of the mechanism, that we probe in the geminate recombination traces.

The location of the bottom of the conduction band rela-

tive to the top of the valence band of water is equal to the adiabatic band-gap energy. As pointed out by Coe,[3] this deliberately adiabatic definition of the band gap differs from the one used to establish a commonly cited band-gap value of 8.9 eV.[5] The bottom of the conduction band (in the middle of the figure) differs from the adiabatic vacuum level by the solvent polarization energy V_0, which has the same value as above.

B. Nature of the ionization mechanism as a function of energy

Within the above framework, we can begin to understand the rapidly increasing ejection length for excitation energies greater than about 9.5 eV. The change in behavior from lower energies, where the ejection length is roughly constant, indicates that the ionization mechanism undergoes a transformation at this point. The conduction band is not directly accessible by vertical excitation in the low energy range because a significant amount of nuclear reorganization is required to access the conduction band in this region, and the population of highly nonequilibrium ground state geometries that overlap with the final states is vanishingly small. More importantly, for excitation energies below the adiabatic bottom of the conduction band at about 7 eV the electron cannot reach the conduction band at all (see Fig. 6),[2] even though ionization occurs down to the onset for optical absorption at 6.5 eV or below.[7,8]

A leading candidate for the ionization mechanism at very low excitation energies is proton-coupled electron transfer, where nuclear motion after molecular excitation allows the system to attain a favorable geometry for transferring the excited electron into a localized (trap) state below the conduction band of the liquid. Importantly, the proton-coupled electron transfer mechanism bypasses the conduction band of the liquid by ejecting the electron into a solvent trap. The situation is potentially different when the excitation energy exceeds the adiabatic band gap and it is energetically possible for the electron to reach the conduction band indirectly via autoionization of a molecular excited state of water. Similar to the gas phase analog, where an electron is ejected into the vacuum from an electronically bound excited state, autoionization of an excited molecule in solution ejects an electron into the conduction band of the liquid. The rate of autoionization depends on the extent of nuclear and solvent reorganization that needs to take place in order to transfer the electron into the conduction band. In other words, the coupling matrix element is large when only minimal reorganization is needed to reach the conduction band, and it is small when significant nuclear rearrangement is required. Estimates for the autoionization lifetime are not currently available, but are a useful target for theoretical work that will also help determine the relative importance of the autoionization mechanism. Because it must compete with O–H bond dissociation (and the proton-coupled electron transfer mechanism), autoionization undoubtedly plays an increasingly important role as the excitation energy approaches the onset of direct, vertical ionization, where the nuclear configuration changes the least and the autoionization rate is largest. In any event, the ejection length for autoionization can be much larger than it is for proton-coupled electron transfer, because the electron passes through the conduction band prior to solvent trapping in the former mechanism.

The constant electron ejection length below about 9.5 eV can be explained by either the proton-coupled electron transfer mechanism or the autoionization mechanism. In the first case, it is the spatial distribution of trap states that determines the electron ejection length and is therefore independent of the excitation energy.[22] An increase in the number of available trap states with excitation energy explains the exponential increase in the ionization yield at low excitation energies in this picture.[22] On the other hand, the constant ejection length in this range may also be the result of the $\tilde{A}$ and $\tilde{B}$ excited states of water having the same excited molecular orbital. Excitation promotes an electron into the $4a_1$ antibonding (oxygen $3s$ Rydberg-type) orbital in each case, with the only difference being the occupied orbital from which the electron is removed. In the autoionization picture, the Rydberg-type character of the two transitions therefore is similar, terminating on the same diffuse oxygen $3s$ orbital. Although the excitation energy increases from the $\tilde{A}$ state to the $\tilde{B}$ state, the coupling matrix element that governs autoionization from the excited molecular state to the conduction band does not change, because each state corresponds to a different ionization continuum with either a $(1b_1)^{-1}$ or a $(3a_1)^{-1}$ cationic core. In other words, the increase in energy does not improve the Franck-Condon overlap of the ground state with the final conduction band states.

The electron ejection length increases most dramatically as a function of excitation energy above 9.5 eV, where two important changes are likely taking place. First, the character of the excited molecular electronic state rapidly changes as higher Rydberg-type orbitals are increasingly likely to be excited. The higher Rydberg orbitals are more diffuse[18,39,40] and, at least in the gas phase, are not directly dissociative.[38] Moreover, with the transitions to higher Rydberg-type states once again involving promotion from the $1b_1$ molecular orbital, nonadiabatic coupling of the excited state to the lowest ionization continuum [corresponding to the $(1b_1)^{-1}$ cationic core] improves dramatically because of the decreasing need for nuclear reorganization as the excitation energy approaches the ionization continuum.

The second important change for excitation above 9.5 eV is that direct optical coupling to the conduction band becomes possible, and the direct ionization mechanism may play an increasingly important role as the excitation energy increases. The direct ionization mechanism requires an optical transition directly from the valence band to the conduction band of liquid water, unlike autoionization, where the electron is bound to the molecule immediately after excitation. Because the direct process is closely related to the production of photoelectrons in the vacuum, the photoelectron spectrum provides a useful reference. The peak in the photoelectron spectrum in Fig. 5(b) gives the most probable excitation energy, 11.2 eV, for ejecting an electron from the $1b_1$ highest occupied orbital of liquid water into the vacuum with zero kinetic energy in the outgoing electron.[26] Combining that energy and the estimate[2] that V_0 is in the range from

−0.12 to 0.0 eV implies that vertical transitions to the conduction band are most likely for excitation energies higher than ~11 eV and that significant transition probability for a direct transition to the conduction band should occur only above 9.8–9.9 eV. This estimate does not reveal the relative absorption cross sections for bound-to-free transitions directly to the conduction band versus transitions to electronically bound, autoionizing molecular states. (Autoionizing states do not contribute to the photoelectron spectrum because the generation of photoelectrons from nonresonant excitation of such states is not possible.) The character of the vertically excited state distinguishes autoionization from direct ionization.

The increase in the average ejection length from 9.5 to 12.4 eV may come from the increasing direct optical coupling to the conduction band in this range and from the fact that the final state of the electron has greater kinetic energy in the conduction band. However, it is highly likely that autoionization from bound Rydberg-type states continues to play a role above the onset for direct vertical ionization (9.8–9.9 eV), because of strong coupling of these states to the conduction band. Potentially, the pathways could be distinguished by differences in the delayed appearance of trapped solvated electrons.[47] Clearly, improved knowledge of the respective absorption cross sections are needed to unravel the relative contributions of direct ionization and autoionization, but our primary conclusion is that the conduction band plays an increasingly important role in the ionization mechanism (through either direct ionization or autoionization) as the excitation energy increases above 9.5 eV.

An alternate picture to explain the increasing ejection length comes from consideration of the increasing size of the vertically excited state wave function.[47] In this picture, the spatial extent of the vertically excited wave function limits the ejection length by limiting the volume within which the electron can travel before it is trapped by the solvent. Thus, the increasing $\langle r_0 \rangle$ with excitation energy comes from increasing the size of the wave function. A larger wave function may be the result of exciting more diffuse Rydberg orbitals or additional mixing of conduction band character into the wave function at higher excitation energies. The advantage of this description is that the same picture can be used regardless of whether the initial excited state is best described as a superposition of plane waves in the conduction band (direct ionization) or as a molecular wave function on the initially excited water molecule that is weakly coupled to the continuum (autoionization). In the latter case, Keszei and Jay-Gerin[48] suggest that such "excitons" are the liquid phase analogs of Rydberg states in the isolated molecule and that these excited states are very diffuse in liquid water. Recent calculations confirm that the excited state wave functions are indeed diffuse,[49] and that even the first excited state includes delocalized electron density on nearby water molecules in ice.[50]

C. Isotope dependence of the ejection length

Comparing the electron ejection length in H_2O and D_2O potentially provides additional information on the changing nature of the ionization mechanism with increasing energy. The average ejection length is consistently shorter by about 0.3 nm in D_2O than it is in H_2O at all of the excitation energies that we study. In the simplest picture, the different vibrational zero-point energies of the two molecules affect the energy dependence of the ejection length by changing the transition energies between the ground and excited electronic states.[6,22] Using the optical absorption spectrum as a probe of this energy shift indicates that the first electronic absorption band is higher in energy by about 0.16 eV for the deuterated liquid.[51] If the zero-point energies were the only reason that the ejection lengths are different in the two liquids, and assuming that the zero-point energy difference is similar for transitions to higher excited states as well, then simply shifting the D_2O data in Fig. 4 to lower energy by that amount would bring them in line with the H_2O points. Importantly, this shift is not sufficient to explain the difference in the ejection lengths that we observe, and, instead, a shift of about 0.35–0.4 eV is necessary. This is roughly the same shift that Sander *et al.*[6] noted for their result at 10 eV excitation and is strikingly similar to the 0.35 eV energy shift of the ionization quantum yield from H_2O to D_2O.[22] The additional shift beyond the zero-point energy effect indicates that isotopic substitution influences the electron ejection length in the two liquids in a more profound manner than to simply shift the amount of available energy.

The impact of isotopic substitution on various ionization mechanisms has previously been discussed in the literature.[4,6,22] In the proton-coupled electron transfer mechanism, for instance, the ejection length should be largely independent of the isotopic composition of liquid water, because it is the concentration of trap sites that determines that length, and should not be very different in D_2O than it is in H_2O.[22] On the other hand, it is difficult to say how isotopic substitution impacts the ejection length for autoionization, where coupling between the electronic and nuclear degrees of freedom is important. One might expect that different Franck-Condon factors lead to different autoionization rates in the two isotopes and, therefore, different efficiencies compared to other deactivation pathways. Although Sander *et al.*[6] point out that the rate (and efficiency) of autoionization does not directly impact the ejection length of the electron, the competition among different ionization pathways depends on their relative rates (i.e., Franck-Condon factors) and could potentially alter the ejection length. Clearly, the development of a theoretical framework for autoionization in liquid water will help a great deal to understand the influence of the different isotopes on the electron ejection mechanism.

An additional complication is that the isotopic composition of the liquid is likely to influence the ejection length of electrons that pass through the conduction band, regardless of the ejection mechanism. The distance that an electron travels in the conduction band before the solvent traps it depends on how efficiently inelastic scattering dissipates the excess kinetic energy[52,53] and is different for H_2O and D_2O.[54–56] Even for direct ionization, which is the only mechanism where nuclear motion does not play a primary role in the ionization process, different inelastic scattering efficiencies are likely to give an isotope dependence of the

ejection length. As we discuss below, different energy loss rates for inelastic scattering of an electron in the two liquids have been implicated in the different geminate kinetics following radiolysis,[56–58] although the radiolysis result seems to contrast with our observations following two-photon excitation in the range of 8.3–12.4 eV.

Radiolysis provides a convenient benchmark for high energy ionization because the average excitation energy is much higher than in the present two-photon experiments. A broad range of energies play a role in the radiolysis of liquid water, due to the nonselective nature of the excitation process and the broad energy loss spectrum that peaks near 22 eV and extends above 100 eV.[59] Electrons from primary ionization events with more than about 8–10 eV of excess energy ionize additional water molecules, leading to a high concentration of ionization events in relatively close proximity. Electrons that do not have sufficient energy to ionize additional water molecules ("subexcitation" electrons) instead relax by transferring energy into vibrations, rotations, and collective modes of the solvent until they lose enough energy to become trapped. These low energy (<8 eV) electrons are the ones that are most closely related to the electrons liberated by two-photon ionization, since even the highest excitation energies in our experiment produce electrons with only a few eV of excess energy. The highly nonhomogeneous distribution of ionization products complicates the extraction of an average electron ejection length from the radiolysis experiments, but recent estimates[60–63] suggest that the separation is much larger (6–12 nm) in radiolysis than at even the highest excitation energy in our experiments, where the ejection length is about 4 nm. It is not surprising that the average separation is larger given the higher average excitation energy in radiolysis (greater than 19 eV excitation to produce up to 8 eV electrons), and the fact that the ejection length still appears to be rising at the highest energies in our photolysis data.

Radiolysis experiments that compare the ejection length in H_2O and in D_2O show that the survival probability of electrons is greater in the deuterated solvent.[56–58] A common interpretation of that observation is that electrons travel further in D_2O, because the stretching and bending vibrational frequencies are lower in D_2O than in H_2O and inelastic scattering from the lower energy vibrations is less efficient at dissipating kinetic energy from the electron.[56] Gas phase electron-scattering measurements confirm that the cross section for vibrational excitation of isolated D_2O is smaller than for H_2O,[64] supporting the conclusion that more collisions with D_2O than H_2O are necessary to remove the same amount of kinetic energy from an electron. The rate of energy dissipation is often related to the dielectric response of the liquid as well, suggesting that even electrons with kinetic energy below the vibrational levels of water travel further in D_2O, which has a longer dielectric relaxation time than H_2O.[65,66] The result is that the amplitude of the (theoretical) energy loss spectrum for electrons in the conduction band of H_2O is larger than it is in D_2O for all energies below the electronic excitation threshold.[67]

Contrary to the radiolysis results, as well as the predictions from the vibrational and dielectric dissipation theories for conduction band electrons, we observe that the ejection length is shorter in D_2O than in H_2O for excitation energies up to 12.4 eV. This suggests that either ionization via the conduction band (autoionization or direct ionization) does not play a major role in the two-photon experiments or that the interpretation of the radiolysis result is not as simple as has been proposed in the literature. The broad range of excitation energies and the highly inhomogeneous deposition of energy in radiolysis experiments leads to significant averaging over the kinetics (and over various ionization mechanisms), which complicates interpretation of that data, while the laser experiments take advantage of tunable, monoenergetic excitation energies and well-separated ionization events. Although the electrons from photoionization in our experiments have somewhat lower energy than most electrons produced in radiolysis they nonetheless represent a subset of the low energy electrons playing a role in radiolysis and potentially help to better understand the ionization mechanism in the latter case. In particular, secondary ionization events from electrons with more than about 8 eV of excess energy do not contribute to the kinetics in the photoionization experiments.

It was previously inferred from the different isotope dependence of the ejection lengths for laser ionization versus radiolysis that two-photon excitation up to 12.4 eV leads to autoionization rather than direct ionization.[6,21] However, the photoelectron spectrum suggests that direct excitation into the conduction band may also occur for excitation energies down to 11 eV, and that the competition between direct ionization and autoionization in the two-photon experiments depends on the nature of the vertically excited state. This once again highlights the need for additional theoretical and experimental efforts to directly reveal the character of the excited state. In either case, it is evident that the conduction band plays an increasingly important role in the ionization mechanism as excitation energies approach and exceed 9.5 eV and that a direct ionization channel is fully accessible by 11 eV. Additional channels from direct ionization of lower lying water molecular orbitals may also contribute above 13 eV.

V. SUMMARY

The geminate kinetics following two-photon ionization of liquid water reveal the ejection length of the nascent electron for excitation energies ranging from 8.3 to 12.4 eV. The average initial separation of the electron from its hydronium ion and hydroxyl radical counterparts increases monotonically from about 0.9 to nearly 4 nm across this energy range, with the increase being most rapid above roughly 9.5 eV. We interpret the increasing ejection length above 9.5 eV as an indication that the electron passes through the conduction band of the liquid. An autoionization mechanism probably plays a role throughout the range from 9 to 12 eV, where there are likely to be several diffuse Rydberg-type states and the conduction band is accessible with only minimal nuclear reorganization. The amount of nuclear reorganization that is necessary for autoionization decreases as the excitation energy increases up to about 11 eV, although vertical excitation

of electrons from the ground state directly into the conduction band of the liquid may also be important at that energy and above. A more complete theoretical picture of the vertically excited state is needed in order to fully distinguish between the autoionization and direct ionization by determining the relative absorption cross sections for exciting electronically bound versus free upper states.

The close agreement of the energy range over which the electron ejection distance in the liquid phase rises steeply with the range over which the liquid photoelectron spectrum has a large vertical transition probability to vacuum is in agreement with the assignment of Coe *et al.* that V_0 is very small for liquid water. Isotopic substitution reveals that the average electron ejection length in liquid D_2O is consistently shorter than in H_2O by about 0.3 nm at all excitation energies. Because this behavior is opposite of the isotope effect inferred from radiolysis experiments, we argue that this highlights the value of energy selective laser ionization experiments to dissect the fundamental events of radiolysis by removing energy averaging and simplifying the initial distribution of ionization products. Additional experiments to systematically study the energy dissipation and solvent trapping of electrons with even higher excess energy in the conduction band are still needed. In addition, our results may justify a renewed examination of how radiolysis trapping lengths are interpreted and simulated.

ACKNOWLEDGMENTS

The authors thank B. Winter for providing the photoelectron spectrum in Fig. 5(b) and for helpful comments about the manuscript. The authors are also grateful to I. A. Shkrob, C. D. Jonah, S. M. Pimblott, D. M. Bartels, and L. Sanche for many helpful discussions, and to J. V. Coe for sharing manuscripts ahead of publication. The work at Argonne National Laboratory was supported by the Office of Science, U.S. Department of Energy, under Contract No. W-31-109-ENG-38. The work at USC is supported by the National Science Foundation (CHE-0311814) and the David and Lucile Packard Foundation.

[1] B. C. Garrett, D. A. Dixon, D. M. Camaioni *et al.*, Chem. Rev. (Washington, D.C.) **105**, 355 (2005).
[2] J. V. Coe, A. D. Earhart, M. H. Cohen, G. J. Hoffman, H. W. Sarkas, and K. H. Bowen, J. Chem. Phys. **107**, 6023 (1997).
[3] J. V. Coe, Int. Rev. Phys. Chem. **20**, 33 (2001).
[4] P. Han and D. M. Bartels, J. Phys. Chem. **94**, 5824 (1990).
[5] A. Bernas, C. Ferradini, and J. P. Jay-Gerin, Chem. Phys. **222**, 151 (1997).
[6] M. U. Sander, M. S. Gudiksen, K. Luther, and J. Troe, Chem. Phys. **258**, 257 (2000).
[7] J. W. Boyle, J. A. Ghormley, C. J. Hochanadel, and J. F. Riley, J. Phys. Chem. **73**, 2886 (1969).
[8] D. N. Nikogosyan, A. A. Oraevsky, and V. I. Rupasov, Chem. Phys. **77**, 131 (1983).
[9] Vertical excitation implies that the nuclei are frozen on the time scale of the transition; we use the term direct ionization for a process in which vertical excitation places the electron directly into the conduction band.
[10] T. Goulet and J. P. Jay-Gerin, J. Chem. Phys. **96**, 5076 (1992).
[11] S. M. Pimblott, J. Phys. Chem. **95**, 6946 (1991).
[12] R. A. Crowell and D. M. Bartels, J. Phys. Chem. **100**, 17940 (1996).
[13] R. A. Crowell, R. Lian, I. A. Shkrob, J. Qian, D. A. Oulianov, and S. Pommeret, J. Phys. Chem. A **108**, 9105 (2004).
[14] M. U. Sander, K. Luther, and J. Troe, J. Phys. Chem. **97**, 11489 (1993).
[15] M. U. Sander, K. Luther, and J. Troe, Ber. Bunsenges. Phys. Chem. **97**, 953 (1993).
[16] A. Reuther, A. Laubereau, and D. N. Nikogosyan, J. Phys. Chem. **100**, 16794 (1996).
[17] J. Peon, G. C. Hess, J. M. L. Pecourt, T. Yuzawa, and B. Kohler, J. Phys. Chem. A **103**, 2460 (1999).
[18] C. L. Thomsen, D. Madsen, S. R. Keiding, J. Thogersen, and O. Christiansen, J. Chem. Phys. **110**, 3453 (1999).
[19] D. Madsen, C. L. Thomsen, J. Thogersen, and S. R. Keiding, J. Chem. Phys. **113**, 1126 (2000).
[20] J. A. Kloepfer, V. H. Vilchiz, V. A. Lenchenkov, A. C. Germaine, and S. E. Bradforth, J. Chem. Phys. **113**, 6288 (2000).
[21] R. Lian, D. A. Oulianov, I. A. Shkrob, and R. A. Crowell, Chem. Phys. Lett. **398**, 102 (2004).
[22] D. M. Bartels and R. A. Crowell, J. Phys. Chem. A **104**, 3349 (2000).
[23] F. H. Long, H. Lu, and K. B. Eisenthal, Chem. Phys. Lett. **160**, 464 (1989).
[24] Y. Gauduel, S. Pommeret, A. Migus, and A. Antonetti, J. Phys. Chem. **95**, 533 (1991).
[25] R. A. Crowell and D. M. Bartels, J. Phys. Chem. **100**, 17713 (1996).
[26] B. Winter, R. Weber, W. Widdra, M. Dittmar, M. Faubel, and I. V. Hertel, J. Phys. Chem. A **108**, 2625 (2004).
[27] F.-Y. Jou and G. R. Freeman, J. Phys. Chem. **83**, 2383 (1979).
[28] A. E. Jailaubekov and S. E. Bradforth, Appl. Phys. Lett. **87**, 021107 (2005).
[29] M. J. Tauber, R. A. Mathies, X. Y. Chen, and S. E. Bradforth, Rev. Sci. Instrum. **74**, 4958 (2003).
[30] V. H. Vilchiz, J. A. Kloepfer, A. C. Germaine, V. A. Lenchenkov, and S. E. Bradforth, J. Phys. Chem. A **105**, 1711 (2001).
[31] R. Lian, R. A. Crowell, and I. A. Shkrob, J. Phys. Chem. A **109**, 1510 (2005).
[32] Y. Gauduel, S. Pommeret, A. Migus, and A. Antonetti, J. Phys. Chem. **93**, 3880 (1989).
[33] See Ref. 19 for a systematic analysis of how the uncertainty in the fit parameters affects the values that we obtain for the average ejection length.
[34] F. H. Long, H. Lu, X. L. Shi, and K. B. Eisenthal, Chem. Phys. Lett. **185**, 47 (1991).
[35] The authors of Ref. 6 mistakenly reported that Ref. 25 examines the isotope dependence for a range of excitation energies, but, in fact, the comparison was made only for 8 eV excitation.
[36] J. M. Heller, Jr., R. N. Hamm, R. D. Birkhoff, and L. R. Painter, J. Chem. Phys. **60**, 3483 (1974).
[37] R. Schinke, *Photodissociation Dynamics* (Cambridge University Press, Cambridge, 1993).
[38] P. Guertler, V. Saile, and E. E. Koch, Chem. Phys. Lett. **51**, 386 (1977).
[39] O. Christiansen, T. M. Nymand, and K. V. Mikkelsen, J. Chem. Phys. **113**, 8101 (2000).
[40] B. D. Bursulaya, J. Jeon, C. N. Yang, and H. J. Kim, J. Phys. Chem. A **104**, 45 (2000).
[41] B. Winter and M. Faubel, Chem. Rev. (Washington, D.C.) **106**, 1176 (2006).
[42] P. Delahay and K. Von Burg, Chem. Phys. Lett. **83**, 250 (1981).
[43] J. V. Coe, S. T. Arnold, J. G. Eaton, G. H. Lee, and K. H. Bowen, J. Chem. Phys. (in press).
[44] J. V. Coe, S. M. Williams, and K. H. Bowen, J. Chem. Phys. (submitted).
[45] P. C. do Couto, S. G. Estacio, and B. J. C. Cabral, J. Chem. Phys. **123**, 054510 (2005).
[46] B. Brena, D. Nordlund, M. Odelius, H. Ogasawara, A. Nilsson, and L. G. M. Pettersson, Phys. Rev. Lett. **93**, 148302 (2004).
[47] P. Kambhampati, D. H. Son, T. W. Kee, and P. F. Barbara, J. Phys. Chem. A **106**, 2374 (2002).
[48] E. Keszei and J. P. Jay-Gerin, Can. J. Chem. **70**, 21 (1992).
[49] M. Boero, M. Parrinello, K. Terakura, T. Ikeshoji, and C. C. Liew, Phys. Rev. Lett. **90**, 226403 (2003).
[50] P. H. Hahn, W. G. Schmidt, K. Seino, M. Preuss, F. Bechstedt, and J. Bernholc, Phys. Rev. Lett. **94**, 037404 (2005).
[51] J. M. Heller, Jr., R. D. Birkhoff, and L. R. Painter, J. Chem. Phys. **67**, 1858 (1977).
[52] J. Meesungnoen, J. P. Jay-Gerin, A. Filali-Mouhim, and S. Mankhetkorn, Radiat. Res. **158**, 657 (2002).
[53] M. Michaud, A. Wen, and L. Sanche, Radiat. Res. **159**, 3 (2003).
[54] V. V. Konovalov, A. M. Raitsimring, Y. D. Tsvetkov, and V. A. Benderskii, Chem. Phys. **93**, 163 (1985).

[55] V. V. Konovalov, A. M. Raitsimring, and Y. D. Tsvetkov, Radiat. Phys. Chem. **32**, 623 (1988).
[56] A. C. Chernovitz and C. D. Jonah, J. Phys. Chem. **92**, 5946 (1988).
[57] C. D. Jonah and A. C. Chernovitz, Can. J. Phys. **68**, 935 (1990).
[58] D. M. Bartels, D. Gosztola, and C. D. Jonah, J. Phys. Chem. A **105**, 8069 (2001).
[59] H. Hayashi, N. Watanabe, Y. Udagawa, and C. C. Kao, Proc. Natl. Acad. Sci. U.S.A. **97**, 6264 (2000).
[60] S. M. Pimblott and J. A. LaVerne, J. Phys. Chem. A **101**, 5828 (1997).
[61] S. M. Pimblott and A. Mozumder, in *Charged Particle and Photon Interactions with Matter: Chemical, Physicochemical, and Biological Consequences with Applications*, edited by A. Mozumder and Y. Hatano (Dekker, New York, 2004).
[62] J. A. LaVerne, Radiat. Res. **153**, 487 (2000).
[63] J. Meesungnoen and J. P. Jay-Gerin, J. Phys. Chem. A **109**, 6406 (2005).
[64] C. Szmytkowski, K. Maciag, P. Koenig, A. Zecca, S. Oss, and R. Grisenti, Chem. Phys. Lett. **179**, 114 (1991).
[65] I. Rips and M. I. Urbakh, J. Chem. Phys. **95**, 2975 (1991).
[66] I. Rips and R. J. Silbey, J. Chem. Phys. **94**, 4495 (1991).
[67] S. V. Stepanov and V. M. Byakov, Nucl. Instrum. Methods Phys. Res. B **221**, 235 (2004).